Weak-field asymptotic theory of tunneling ionization from nearly degenerate states

Pavel K. Samygin,[1] Toru Morishita,[2] and Oleg I. Tolstikhin[1]
[1]*Moscow Institute of Physics and Technology, Dolgoprudny 141700, Russia*
[2]*Institute for Advanced Science, The University of Electro-Communications, 1-5-1 Chofu-ga-oka, Chofu-shi, Tokyo 182-8585, Japan*

(Received 22 June 2018; published 4 September 2018)

The weak-field asymptotic theory (WFAT) of tunneling ionization in a static electric field is limited by the assumption that tunneling occurs from an isolated state in a compact atomic or molecular system. In this paper, we generalize the WFAT in two directions: to the cases when tunneling ionization occurs from (i) nearly degenerate states separated by a small energy distance ΔE in compact systems, and (ii) an isolated state in heteronuclear diatomic molecules at large internuclear distances R. The weak-field asymptotic formulas for the ionization rates in these two cases are obtained. The asymptotics are uniform with respect to ΔE and R and for sufficiently large ΔE and small R, respectively, reduce to the previously known WFAT rate formula. By combining the two asymptotics, we obtain a formula for the ionization rates from the nearly degenerate $1s\sigma_g$ and $2p\sigma_u$ states of a homonuclear molecular ion H_2^+ at large internuclear distances, which is of particular interest for applications in strong-field physics. The analytical results are illustrated by calculations for several atomic and molecular models.

DOI: 10.1103/PhysRevA.98.033401

I. INTRODUCTION

The description of tunneling ionization from a bound state in a given potential caused by an external static electric field is one of the basic problems in quantum mechanics. If the field is sufficiently weak compared to a critical field F_c at which over-the-barrier ionization becomes accessible, the ionization rate can be sought as an asymptotic expansion in the field strength F. Such an approach was initiated in Ref. [1], where the leading-order term in the expansion of the ionization rate from the ground state in the Coulomb potential was obtained. This result was then generalized to an arbitrary state in an arbitrary central atomic potential [2], to excited states in the Coulomb potential [3,4], and to the first-order [5] and higher-order [6] terms in the expansion for the Coulomb potential. More recently, the asymptotic approach was reformulated on the basis of the method of expansion in parabolic channels [7]. This enabled one to generalize it to arbitrary molecular potentials without any symmetry in the leading-order approximation [7] and including the first-order terms [8], which became known as the weak-field asymptotic theory (WFAT). The WFAT was further generalized to many-electron systems in the leading-order approximation [9] and including the first-order terms [10,11], but in this paper we discuss only the one-electron theory. We mention that other analytical approaches to the problem of tunneling ionization [12–15] were also proposed.

The development of the WFAT originally was and continues to be motivated by applications in strong-field physics [16]. The ionization of atoms and molecules by strong laser fields is often treated in the single-active-electron approximation in which the interaction of the active electron with the parent ion is modeled by an effective potential. In the adiabatic regime, when the laser photon energy is much smaller than the energy distance ΔE between the initial and the nearest excited electronic states, the interaction of the active electron with a laser field can be treated as if the field were static and equal to the instantaneous value of the laser field [17]. For atoms and molecules in the ground state, ΔE is of the order of the ionization potential $I_p \sim 0.5$ a.u., so for a typical wavelength of $\lambda \sim 800$ nm (photon energy of $\hbar\omega \sim 0.06$ a.u.) the adiabatic approximation holds. The quantitative performance of the adiabatic approximation in predicting total ionization yields [18,19] and complete description of photoelectron momentum distributions [17,20,21] has been multiply confirmed by comparison with exact solutions of the time-dependent Schrödinger equation. Furthermore, for typical laser intensities $I \sim 10^{13}$–10^{14} W/cm^2 the field amplitude $F \sim 0.02$–0.05 a.u. is smaller than a typical critical field $F_c \sim 0.1$ a.u. This justifies the success of the WFAT in applications to the analysis of ionization in strong-field experiments [22–25].

The external static electric field causing tunneling ionization simultaneously shifts the energy of the state. The present version of the WFAT [7] is limited by the assumption that this Stark shift is small compared to ΔE. In other words, the WFAT treats tunneling ionization from an isolated state which is well separated in energy from the other states of the unperturbed system. One exception is the results for the hydrogen atom in degenerate excited states [3,4] reproduced within the WFAT [7]. However, the Coulomb potential presents a very special case since the Schrödinger equation describing tunneling in this case allows separation of variables in parabolic coordinates [1], which amounts to exact decoupling of parabolic channels within the WFAT [7]. The ionization rates obtained in Refs. [3,4] are that of parabolic states of hydrogen. These are the correct zeroth-order eigenstates in an electric field [1], which suggests a guiding idea for the present study. In this paper, we generalize the WFAT to the case when tunneling ionization occurs from a group of nearly degenerate states of the unperturbed system which can be mixed by even a weak external field. The physical effect we wish to investigate is how the mixing of the states affects their ionization rates.

One of the original goals of this study was to consider tunneling ionization from the nearly degenerate $1s\sigma_g$ and $2p\sigma_u$ states of H_2^+ at large internuclear distances R. It turned out that in order to treat this system, in addition to the generalization mentioned above a generalization of the WFAT in another direction is needed. The present version of the WFAT [7] treats tunneling ionization from a compact system. The case of a system of large spatial extent, e.g., a dissociating molecule, requires special treatment. The system we keep in mind is a molecule undergoing Coulomb explosion into several fragments separated by large distances. As an electron initially localized at one of the fragments tunnels and leaves the system being driven by the external field, an effective charge it feels varies from that of the parent fragment ion to the sum of charges of all fragments. The two charges are generally different, since the other fragments may be charged. The ionization rate depends on the parent ion charge, so the variation of the charge affects its value. In this paper, we show how to take this effect into account within the WFAT. The combination of the two generalizations enables us to consider tunneling ionization of dissociating H_2^+.

The developments of the WFAT outlined above, and our interest in H_2^+ at large internuclear distances in particular, are again motivated by possible applications in strong-field physics. One could argue that for systems with small energy spacing ΔE of interest here the adiabatic approximation may break down, which is of course true. However, the results of this paper still contribute to the theory of tunneling ionization in a static field. Moreover, new laser sources progressing towards longer wavelengths continue to appear [26], so the present results may find applications in the future.

The paper is organized as follows. In Sec. II, we summarize basic equations of the WFAT and illustrate its performance for tunneling ionization from an isolated state in a compact system. In Sec. III, we present the generalization to the case when tunneling ionization occurs from nearly degenerate states in a compact system. In Sec. IV, the generalization to the case when tunneling ionization occurs from an isolated state in a heteronuclear diatomic molecule at large internuclear distances is developed. In Sec. V, the results of the two previous sections are combined to obtain tunneling ionization rates from the nearly degenerate $1s\sigma_g$ and $2p\sigma_u$ states of H_2^+ at large internuclear distances. The weak-field asymptotic formulas for the ionization rates obtained in Secs. III–V are illustrated and validated by calculations. Section VI concludes the paper.

II. TUNNELING IONIZATION FROM AN ISOLATED STATE

In this section, we summarize basic equations of the WFAT for tunneling ionization from an isolated state [7], which is needed to set up a framework for the following generalizations. The Schrödinger equation describing an atom or molecule interacting with a static uniform electric field $\mathbf{F} = F\mathbf{e}_z$, $F \geqslant 0$, in the single-active-electron approximation reads (atomic units are used throughout)

$$\left[-\tfrac{1}{2}\Delta + V(\mathbf{r}) + Fz - E\right]\psi(\mathbf{r}) = 0. \tag{1}$$

The potential is assumed to satisfy

$$V(\mathbf{r})|_{r\to\infty} = -\frac{Z}{r} + O(r^{-2}), \tag{2}$$

where Z is the total charge of the parent ion. In the absence of the field, $F = 0$, Eq. (1) has a solution with real energy $E_0 < 0$ and wave function $\psi_0(\mathbf{r})$ representing the unperturbed bound state of the active electron. For $F > 0$, this state turns into a Siegert state (SS) in an electric field [27–29]. The SS satisfies Eq. (1) subject to outgoing-wave boundary conditions in the asymptotic region $z \to -\infty$. The SS eigenvalue is complex,

$$E = \mathcal{E} - \tfrac{i}{2}\Gamma, \tag{3}$$

and defines the Stark-shifted energy $\mathcal{E}$ and ionization rate Γ of the state, and the outgoing-wave tail of the SS eigenfunction $\psi(\mathbf{r})$ describes tunneled electrons. All properties of the system related to tunneling ionization can be expressed in terms of the SS. Within the WFAT, they are obtained in the form of asymptotic expansions in F for

$$F \to 0. \tag{4}$$

In this paper we discuss only the ionization rate, since it is of main interest for applications.

In the weak-field limit (4), one could attempt to solve Eq. (1) using perturbation theory. This approach results in the expansions [1]

$$E = E_0 - \mu_z F + O(F^2), \tag{5a}$$

$$\psi(\mathbf{r}) = \psi_0(\mathbf{r}) + O(F^1), \tag{5b}$$

where

$$\mu_z = -\int \psi_0(\mathbf{r}) z \psi_0(\mathbf{r})\, d\mathbf{r} \tag{6}$$

is the z component of the dipole moment in the unperturbed state. However, Eqs. (5) do not account for tunneling ionization. Indeed, all terms in Eq. (5a) are real and all terms in Eq. (5b) vanish at $r \to \infty$. These power series expansions fail to reproduce the imaginary part of E and the outgoing-wave tail of $\psi(\mathbf{r})$ which are exponentially small in F. Yet perturbation theory plays a role in implementing WFAT since coefficients in the WFAT expansion of the ionization rate are expressed in terms of the properties of the unperturbed system appearing in Eqs. (5). In the following, we assume that these properties are known.

In the WFAT, Eq. (1) is treated in parabolic coordinates $\xi = r + z$, $\eta = r - z$, and $\varphi = \arctan(y/x)$ [1]. The solution representing the SS is sought in the form [7]

$$\psi(\mathbf{r}) = \eta^{-1/2} \sum_\nu f_\nu(\eta)\Phi_\nu(\xi, \varphi), \tag{7}$$

where

$$\Phi_\nu(\xi, \varphi) = \phi_\nu(\xi)\, \frac{e^{im\varphi}}{\sqrt{2\pi}} \tag{8}$$

are parabolic channel functions enumerated by the set of parabolic quantum numbers

$$\nu = (n_\xi, m), \quad n_\xi = 0, 1, \ldots, \quad m = 0, \pm 1, \ldots, \tag{9}$$

$\phi_\nu(\xi)$ are solutions to the eigenvalue problem

$$\left[\frac{d}{d\xi}\xi\frac{d}{d\xi} - \frac{m^2}{4\xi} + Z + \frac{E\xi}{2} - \frac{F\xi^2}{4} - \beta_\nu\right]\phi_\nu(\xi) = 0, \tag{10a}$$

$$\phi_\nu(\xi)|_{\xi\to 0} \propto \xi^{|m|/2}, \quad \phi_\nu(\xi)|_{\xi\to\infty} = 0, \tag{10b}$$

normalized by the condition

$$\int_0^\infty \phi_{n_\xi m}(\xi)\phi_{n'_\xi m}(\xi)\,d\xi = \delta_{n_\xi n'_\xi}, \tag{11}$$

and β_ν are the corresponding separation constants. The channel functions (8) are orthonormal with respect to the inner product

$$\langle\Phi_\nu|\Phi_{\nu'}\rangle \equiv \int_0^\infty\int_0^{2\pi} \Phi_{\bar\nu}(\xi,\varphi)\Phi_{\nu'}(\xi,\varphi)\,d\xi d\varphi = \delta_{\nu\nu'}, \tag{12}$$

where $\bar\nu = (n_\xi, -m)$ and $\nu' = (n'_\xi, m')$. In the limit (4), the solutions to Eqs. (10) can be found using perturbation theory,

$$\beta_\nu = \beta_\nu^{(0)} + O(F^1), \tag{13a}$$

$$\phi_\nu(\xi) = \phi_\nu^{(0)}(\xi) + O(F^1). \tag{13b}$$

The field-free terms in these expansions are given by [7]

$$\beta_\nu^{(0)} = Z - \varkappa\left(n_\xi + \frac{|m|+1}{2}\right), \tag{14a}$$

$$\phi_\nu^{(0)}(\xi) = \varkappa^{1/2}(\varkappa\xi)^{|m|/2}e^{-\varkappa\xi/2}\sqrt{\frac{n_\xi!}{(n_\xi+|m|)!}}\,L_{n_\xi}^{(|m|)}(\varkappa\xi), \tag{14b}$$

where $\varkappa = \sqrt{-2E_0}$ and $L_n^{(\alpha)}(x)$ are the generalized Laguerre polynomials [30]. Substituting Eq. (7) into Eq. (1), one obtains a set of ordinary differential equations defining the coefficient functions $f_\nu(\eta)$ [7,8],

$$\left[\frac{d^2}{d\eta^2} + \frac{F\eta}{4} + \frac{E}{2} + \frac{\beta_\nu}{\eta} + \frac{1-m^2}{4\eta^2}\right]f_\nu(\eta) + \frac{1}{\eta}\sum_{\nu'} w_{\nu\nu'}(\eta)f_{\nu'}(\eta) = 0, \tag{15}$$

where

$$w_{\nu\nu'}(\eta) = \langle\Phi_\nu|[Z(\mathbf{r}) - Z]|\Phi_{\nu'}\rangle \tag{16}$$

is a coupling matrix and

$$Z(\mathbf{r}) = -rV(\mathbf{r}) \tag{17}$$

is an effective position-dependent charge. The asymptotic region $z \to -\infty$, where electrons released from the system fly away driven by the field, corresponds to $\eta \to \infty$. As follows from Eq. (2), the matrix (16) vanishes in this region, Eqs. (15) become decoupled, and we present them in the form

$$\left[\frac{d^2}{d\eta^2} + \frac{F\eta}{4} + \frac{E}{2} + \frac{\beta_\nu}{\eta} + O(\eta^{-2})\right]f_\nu(\eta) = 0. \tag{18}$$

The outgoing-wave solution to this equation satisfies

$$f_\nu(\eta)|_{\eta\to\infty} = \frac{2^{1/2}f_\nu}{(F\eta)^{1/4}}\exp\left[\frac{iF^{1/2}\eta^{3/2}}{3} + \frac{iE\eta^{1/2}}{F^{1/2}}\right], \tag{19}$$

where f_ν is the ionization amplitude in channel ν. In the limit (4), the total ionization rate from Eq. (3) is given by [7]

$$\Gamma = \sum_\nu \Gamma_\nu, \quad \Gamma_\nu = |f_\nu|^2, \tag{20}$$

where Γ_ν is the partial rate of ionization in channel ν. The problem of finding the rate Γ thus reduces to evaluating the amplitudes f_ν.

The perturbation theory solution (5b) also can be expanded in parabolic channels, as in Eq. (7). In particular, the unperturbed bound state can be presented in the form

$$\psi_0(\mathbf{r}) = \eta^{-1/2}\sum_\nu g_\nu(\eta)\Phi_\nu^{(0)}(\xi,\varphi), \tag{21}$$

where $\Phi_\nu^{(0)}(\xi,\varphi)$ are the field-free channel functions obtained by substituting Eq. (14b) into Eq. (8). We use a different notation for the coefficient functions in Eq. (21), to emphasize that they satisfy different asymptotic boundary conditions. For $F = 0$, one obtains from Eq. (18)

$$g_\nu(\eta)|_{\eta\to\infty} = g_\nu\eta^{\beta_\nu^{(0)}/\varkappa}e^{-\varkappa\eta/2}, \tag{22}$$

where g_ν is the asymptotic coefficient in channel ν.

The ionization amplitudes f_ν are found by matching the *outer* outgoing-wave solution defined by Eqs. (7) and (19) with the *inner* perturbation theory solution given by Eq. (5b). Let us outline briefly the matching procedure, specifying the intervals of η where the different approximations apply, which is needed for the following. The solutions are matched on the basis of the decoupled equations (18). The decoupling approximation holds at $\eta > \eta_c$, where η_c is the boundary of the coupling or core region. We first discuss the outer solution. The asymptotic form (19) holds at $\eta \gg \eta_t$, where $\eta_t = \varkappa^2/F + O(F^0)$ is the outer turning point for Eq. (18). In the limit (4), the solution to Eq. (18) satisfying Eq. (19) can be obtained in the form of the asymptotic expansion in F. To this end, one should substitute into Eq. (18) perturbation theory expansions (5a) and (13a). The derivation employs standard techniques from asymptotic analysis [31,32]; a similar approach is used in the derivation of the semiclassical approximation [1], but the asymptotic parameters in the two cases are different. The asymptotic expansion can be analytically continued to the region $\eta \ll \eta_t$ up to the point $\eta_{\rm as} = 4|\beta_\nu^{(0)}|/\varkappa^2$, where the fourth term in Eq. (18) becomes comparable with the third term. Thus, the inner boundary of the interval where the weak-field asymptotics of the outer solution is known is $\eta_{\rm in} = \max(\eta_c, \eta_{\rm as})$. Now we discuss the inner solution. The terms containing field in Eq. (18) can be treated as a perturbation. The outer boundary of the interval where perturbation theory applies can be estimated by equating the second and fourth terms in Eq. (18), which gives $\eta_{\rm PT} = 2|\beta_\nu^{(0)}/F|^{1/2}$. It is important to recognize that $\eta_{\rm in} = O(F^0)$, $\eta_{\rm PT} = O(F^{-1/2})$, and $\eta_t = O(F^{-1})$, and hence for sufficiently small F these boundaries satisfy $\eta_{\rm in} \ll \eta_{\rm PT} \ll \eta_t$. The expansions in F of the inner and outer solutions are matched term by term in a region $\eta = O(F^{-1/2})$ lying to the left of $\eta_{\rm PT}$, where both solutions apply. This yields the asymptotic expansion for f_ν. In the leading-order approximation, only terms retained in Eqs. (2), (5), (13), and (18) are needed for the derivation. Further details can be found in Ref. [7]; the result is

$$f_\nu = \frac{g_\nu\varkappa^{1/2}}{2^{1/2}}\left(\frac{4\varkappa^2}{F}\right)^{\beta_\nu^{(0)}/\varkappa}\exp\left[\frac{i\pi}{4} + \frac{i\pi\beta_\nu^{(0)}}{\varkappa} - \varkappa\mu_z - \frac{\varkappa^3}{3F}\right]. \tag{23}$$

The first-order correction to this formula was obtained in Ref. [8], its derivation requires to extend the expansions in Eqs. (2), (5), (13), and (18) to the next term.

Using Eq. (23), one obtains partial ionization rates

$$\Gamma_\nu = |G_\nu|^2 W_\nu(F,\varkappa), \tag{24}$$

where

$$G_\nu = g_\nu e^{-\varkappa\mu_z} \tag{25}$$

is the structure factor and

$$W_\nu(F,\varkappa) = \frac{\varkappa}{2}\left(\frac{4\varkappa^2}{F}\right)^{2Z/\varkappa-2n_\xi-|m|-1} \exp\left(-\frac{2\varkappa^3}{3F}\right) \tag{26}$$

is the field factor. Note that under a shift $\mathbf{r}\to\mathbf{r}+\mathbf{a}$ of the coordinate frame in Eq. (1) the dipole moment (6) and the asymptotic coefficients in Eq. (22) undergo transformations $\mu_z\to\mu_z-a_z$ and $g_\nu\to g_\nu e^{-\varkappa a_z}$. Thus, the structure factor G_ν is invariant under the shift, which qualifies it as the primary property of the system related to tunneling ionization, while each of the two factors on the right-hand side of Eq. (25) is not [7]. The different channels have the same exponential factor but different powers of F in Eq. (26). In the leading-order approximation only the dominant channel corresponding to the lowest power should be retained in the sum (20). In the general case this is the channel with $\nu=(0,0)$, provided that $g_{00}\neq 0$. Thus

$$\Gamma \approx G_{00}^2 W_{00}(F,\varkappa). \tag{27}$$

This approximation holds under the condition

$$F \ll F_c \approx \frac{\varkappa^4}{8|2Z-\varkappa|}, \tag{28}$$

where F_c is the critical field at which over-the-barrier ionization becomes accessible. This condition specifies the meaning of the limit (4).

To illustrate the performance of the WFAT, let us consider tunneling ionization from the ground state of the hydrogen atom. The energy $\mathcal{E}$ and ionization rate Γ for this system as functions of F are shown in Fig. 1. The exact results are obtained from the SS eigenvalue (3) calculated using the method and program developed in Ref. [27]. The same applies to the exact results for the other systems reported below. The energy is compared with the second-order perturbation theory result $\mathcal{E}=-1/2-9F^2/4$ [1] denoted by PT. The rate varies by many orders of magnitude in the interval of F where it was calculated. To eliminate this variation, and thus facilitate comparison with the WFAT on a linear scale, we plot the ratio $\Gamma/W_{00}(F,\varkappa)$. It may be instructive to know the range of the variation of the absolute value of the rate; this is indicated in the figure caption. A similar representation of rates by some ratios accompanied by the indication of the range of their variation is used for the other systems considered below. For the present system $Z=1$, $\varkappa=1$, $\mu_z=0$, and $g_{00}=\sqrt{2}$, so $G_{00}^2=2$ and $W_{00}(F,\varkappa)=2F^{-1}e^{-2/3F}$. The exact rate is compared with the leading-order WFAT result from Eq. (27) given by $\Gamma=4F^{-1}e^{-2/3F}$ [1,3,4,7] and the first-order WFAT result given by $\Gamma=4F^{-1}e^{-2/3F}(1-107F/12)$ [5,6,8] denoted in the figure by WFAT(0) and WFAT(1), respectively. The leading-order approximation overestimates the rate; it works quantitatively only at rather weak fields satisfying (28), where in the present case $F_c\approx 0.125$. The first-order correction considerably improves the WFAT results, making them applicable up to $F\sim F_c$. The behavior of the exact and WFAT rates shown in Fig. 1 is typical for tunneling ionization from an isolated state in atomic [7,8] and molecular [28,33] potentials.

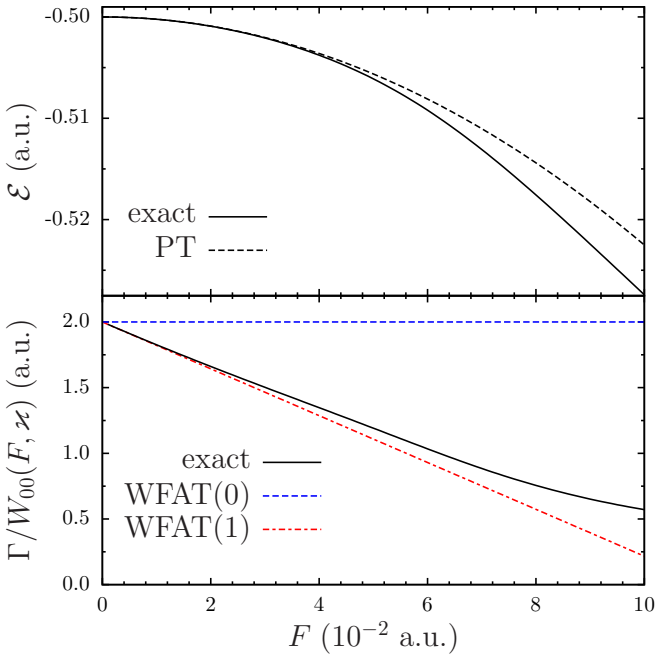

FIG. 1. Energy $\mathcal{E}$ and ionization rate Γ divided by the field factor $W_{00}(F,\varkappa)$, Eq. (26), as functions of field for the ground state of a hydrogen atom. Solid (black) lines show results of accurate calculations. The dashed (black) line in the upper panel shows the second-order perturbation theory results [1]. The dashed (blue) and dash-dotted (red) lines in the lower panel show the leading-order [1,3,4,7] and the first-order [5,6,8] WFAT results, respectively. The rate Γ varies from $\sim 10^{-286}$ at $F=10^{-3}$ to $\sim 10^{-2}$ at $F=10^{-1}$.

III. NEARLY DEGENERATE STATES IN COMPACT SYSTEMS

In this section, we generalize the WFAT to the situation where tunneling ionization occurs from one of a group of nearly degenerate states in a compact atomic or molecular system. Let the system have two closely spaced unperturbed bound states with real energies $E_i<0$ and wave functions $\psi_i(\mathbf{r})$, $i=1,2$; the generalization to a larger number of states is straightforward. For definiteness, we assume that $E_1\leqslant E_2$. The condition that the states are nearly degenerate signifies that there appears a new small parameter $\Delta E=E_2-E_1$ in the problem. Our goal is to obtain the weak-field asymptotics of the ionization rates for these states which is uniform in ΔE, that is, remains valid for any ΔE. To proceed with the derivation, we need to fix the order of ΔE in terms of F. We consider the asymptotics

$$F\to 0, \quad \Delta E = O(F^1). \tag{29}$$

The meaning of the second relation is clarified below. We restrict our treatment to the leading-order approximation in the limit (29).

The main difference of the present situation from the case of an isolated state discussed in the previous section is that

the perturbation theory procedure used to construct the inner solution requires a modification. Namely, instead of dealing with expansions (5), one should solve the corresponding secular equation [1]. In the leading-order approximation of this approach the solution to Eq. (1) is sought in the form $\psi(\mathbf{r}) = c_1\psi_1(\mathbf{r}) + c_2\psi_2(\mathbf{r})$. Substituting this into Eq. (1) leads to the eigenvalue problem

$$\begin{pmatrix} E_1 - \mu_1 F - E & -dF \\ -dF & E_2 - \mu_2 F - E \end{pmatrix}\begin{pmatrix} c_1 \\ c_2 \end{pmatrix} = 0, \tag{30}$$

where

$$\mu_i = -\int \psi_i(\mathbf{r}) z \psi_i(\mathbf{r}) d\mathbf{r} \tag{31}$$

and

$$d = -\int \psi_1(\mathbf{r}) z \psi_2(\mathbf{r}) d\mathbf{r}. \tag{32}$$

The perturbed eigenvalues and eigenfunctions defined by Eq. (30) are denoted by $E_\pm$ and $\psi_\pm(\mathbf{r})$. By our convention $E_+ \geqslant E_-$, so in the limit (4) for a fixed ΔE the states $-$ and $+$ coincide with the states 1 and 2, respectively. We find

$$E_\pm = \tfrac{1}{2}\big[E_1 + E_2 - (\mu_1 + \mu_2)F \pm \sqrt{(\Delta E - \Delta\mu F)^2 + 4d^2F^2}\big] \tag{33}$$

and

$$\psi_-(\mathbf{r}) = \cos\phi\,\psi_1(\mathbf{r}) + \sin\phi\,\psi_2(\mathbf{r}), \tag{34a}$$

$$\psi_+(\mathbf{r}) = -\sin\phi\,\psi_1(\mathbf{r}) + \cos\phi\,\psi_2(\mathbf{r}), \tag{34b}$$

where $\Delta\mu = \mu_2 - \mu_1$, $\phi = \arctan(dF/\Delta)$, and

$$\Delta = \tfrac{1}{2}\big[\Delta E - \Delta\mu F + \sqrt{(\Delta E - \Delta\mu F)^2 + 4d^2F^2}\big]. \tag{35}$$

Thus, the inner solutions in the present case are defined by Eqs. (33) and (34) which replace Eqs. (5). In other words, tunneling ionization occurs from the perturbed states. These states depend on F, and this affects the field dependence of the ionization rates. Note that, due to the second of Eq. (29), the difference between the eigenvalues $E_\pm$ and E_i is $O(F^1)$, and hence remains small at sufficiently weak fields. On the other hand, $\Delta = O(F^1)$, so $\phi = O(F^0)$, which means that the eigenfunctions $\psi_\pm(\mathbf{r})$ can considerably differ from $\psi_i(\mathbf{r})$. In the degenerate case, $\Delta E = 0$, $\psi_\pm(\mathbf{r})$ do not depend on F and represent the correct zeroth-order eigenstates of the unperturbed system [1].

In the leading-order approximation, for matching the inner and outer solutions it is sufficient to consider only the dominant ionization channel $\nu = (0, 0)$; for brevity, we suppress this subscript in the following. It is convenient to introduce a modified notation for the corresponding field-free channel function (8),

$$\Phi(\xi;\varkappa) = \sqrt{\frac{\varkappa}{2\pi}}e^{-\varkappa\xi/2}. \tag{36}$$

According to Eqs. (21) and (22), the unperturbed states satisfy

$$\psi_i(\mathbf{r})|_{\eta\to\infty} = g_i\eta^{Z/\varkappa_i - 1}e^{-\varkappa_i\eta/2}\Phi(\xi;\varkappa_i), \tag{37}$$

where $\varkappa_i = \sqrt{-2E_i}$ and g_i are the asymptotic coefficients. In the present case one cannot expand the perturbed energies (33) in powers of F, as in Eq. (5a). Instead, one should solve Eqs. (10) and (18) with E substituted by $E_\pm$. Then the perturbed states in the matching region $\eta = O(F^{-1/2})$ are given by

$$\psi_\pm(\mathbf{r})|_{\eta=O(F^{-1/2})} = g_\pm\eta^{Z/\varkappa_\pm - 1}e^{-\varkappa_\pm\eta/2}\Phi(\xi;\varkappa_\pm), \tag{38}$$

where $\varkappa_\pm = \sqrt{-2E_\pm}$. The difference between $\varkappa_\pm$ and $\varkappa_i$ is $O(F^1)$, so it can be neglected in the matching region. Then from Eqs. (34) and (37) we obtain

$$g_- = \cos\phi\, g_1 + \sin\phi\, g_2, \tag{39a}$$

$$g_+ = -\sin\phi\, g_1 + \cos\phi\, g_2. \tag{39b}$$

Equation (38) defines the inner solutions to be used in the matching procedure. The rest of the derivation coincides with that in Ref. [7]. We thus obtain the amplitudes of ionization in channel $\nu = (0, 0)$ from the states $\psi_\pm(\mathbf{r})$,

$$f_\pm = \frac{g_\pm\varkappa_\pm^{1/2}}{2^{1/2}}\left(\frac{4\varkappa_\pm^2}{F}\right)^{Z/\varkappa_\pm - 1/2}\exp\left[\frac{i\pi Z}{\varkappa_\pm} - \frac{i\pi}{4} - \frac{\varkappa_\pm^3}{3F}\right]. \tag{40}$$

This result differs from Eq. (23) for the same channel in two respects. First, field-independent quantities $\varkappa$ and g_{00} characterizing the unperturbed state are replaced by field-dependent quantities $\varkappa_\pm$ and $g_\pm$ characterizing the perturbed states. Second, the term with μ_z in the exponent in Eq. (23), originating from the second term in Eq. (5a), is absorbed into the last term in the exponent in Eq. (40). Using Eq. (40), we obtain the ionization rates

$$\Gamma_\pm \approx \Gamma_\pm^{(\mathrm{as})} = g_\pm^2 W_{00}(F, \varkappa_\pm). \tag{41}$$

This formula generalizes Eq. (27) to the case of nearly degenerate states.

In contrast to Eq. (27), where only the field factor (26) contains the dependence on F, Eq. (41) depends on F also through $\varkappa_\pm$ and $g_\pm$. Let us discuss this dependence in more detail. The situation depends on the relation between $\Delta\mu$ and d. We assume that $|\Delta\mu| \ll |d|$, which holds for the models considered in the illustrative calculations below. As can be seen from Eqs. (33) and (35), under this condition one can distinguish two regimes in the variation of the perturbed states with F separated by a field

$$F_d = \frac{\Delta E}{2|d|}, \tag{42}$$

where the Stark splitting $2|d|F$ coincides with the energy distance ΔE between the unperturbed states. At weak fields, $F \ll F_d$, the perturbed states only slightly differ from the unperturbed ones. In this case

$$E_{-,+} = E_{1,2} - \mu_{1,2}F + O(F^2), \tag{43a}$$

$$g_{-,+} = g_{1,2} + O(F^1), \tag{43b}$$

where $-$ and $+$ correspond to 1 and 2, respectively. Substituting this into Eq. (41) and expanding in F, in the leading-order approximation one obtains the previous result (27) applied to

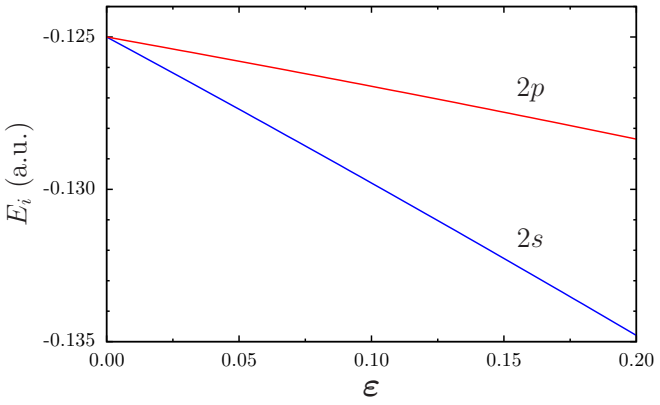

FIG. 2. Energies of the $2s$ and $2p$ bound states in the potential (45) as functions of the screening parameter ε.

each of the two unperturbed states treated as if they were isolated. At stronger fields, $F \gg F_d$, the perturbed states considerably differ from the unperturbed ones. In this case

$$E_\pm = \frac{1}{2}[E_1 + E_2 - (\mu_1 + \mu_2)F] \pm |d|F, \tag{44a}$$

$$g_\pm = \frac{\mp g_1 + g_2}{\sqrt{2}}. \tag{44b}$$

Substituting this into Eq. (41) and expanding in F, one again obtains Eq. (27) with $\varkappa$, μ_z, and g_{00} substituted by $\bar{\varkappa} = \sqrt{-(E_1 + E_2)}$, $(\mu_1 + \mu_2)/2 \mp |d|$, and $g_\pm$, respectively. Formula (41) describes the transition between the two limits. Note that in both limits it is invariant under a shift $\mathbf{r} \to \mathbf{r} + \mathbf{a}$ of the coordinate frame in Eq. (1), because d does not change under the shift. This formula applies in the interval (28), where $\varkappa$ should be substituted by $\bar{\varkappa}$. If $F_d \gtrsim F_c$, in this interval Eq. (41) reduces to Eq. (27), which returns us to the case of an isolated state. Of main interest for the present analysis is therefore the situation where the transition between the two regimes occurs within the interval (28), which is the case if $F_d \ll F_c$. Taking into account Eq. (42), this explains the second of Eqs. (29).

To illustrate the performance of Eq. (41), we consider tunneling ionization from the $2s$ and $2p$ states in the potential

$$V(r) = -\frac{1 + \varepsilon e^{-r}}{r}, \tag{45}$$

where ε is a screening parameter. For $\varepsilon = 0$, the states under consideration are degenerate. For $\varepsilon > 0$, the degeneracy is lifted, but the states remain closely spaced for sufficiently small values of ε. Their energies as functions of ε are shown in Fig. 2. We associate the $2s$ and $2p$ states in the potential (45) with states 1 and 2 in the above discussion, respectively. In the present model $Z = 1$ and $\mu_i = 0$. The signs of $\psi_i(\mathbf{r})$ are chosen in such a way that $g_i > 0$, and consequently $d > 0$.

The energies $\mathcal{E}_\pm$ and ionization rates $\Gamma_\pm$ calculated for this model with $\varepsilon = 0.05$ and 0.2 are shown in Figs. 3 and 4. The corresponding values of the parameters E_i, g_i, and d and the field F_d are given in captions to the figures. The critical field estimated using Eq. (28) is $F_c \approx 5.4\times10^{-3}$ and 5.8×10^{-3} for $\varepsilon = 0.05$ and 0.2, respectively, which explains the interval of field considered in the figures. The exact results are compared

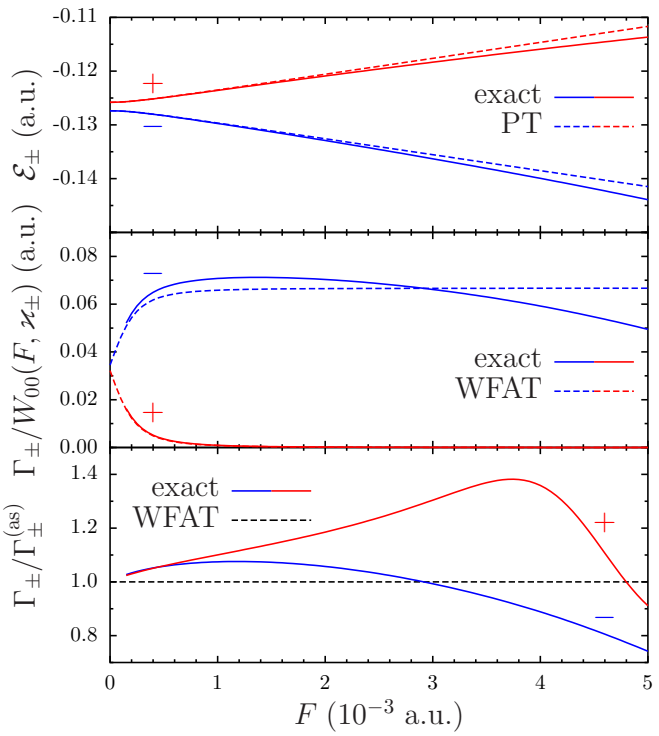

FIG. 3. Energies $\mathcal{E}_\pm$ and ionization rates $\Gamma_\pm$ divided by the field factors $W_{00}(F, \varkappa_\pm)$, in the middle panel, and the WFAT rates $\Gamma_\pm^{(as)}$ defined in Eq. (41), in the bottom panel, as functions of field for the $2s$ and $2p$ states in the potential (45) with $\varepsilon = 0.05$. In this case $E_{2s} = -0.127\,370$, $E_{2p} = -0.125\,795$, $g_{2s} = 0.1857$, $g_{2p} = 0.1794$, and $d = 2.976$, so $F_d = 2.6\times10^{-4}$. Solid lines show results of accurate calculations. Dashed lines in the upper panel show the perturbation theory results from Eq. (33). Dashed lines in the middle and bottom panels show the WFAT results from Eq. (41). Γ_- and Γ_+ vary from $\sim10^{-239}$ and 10^{-234} at $F = 1.5\times10^{-4}$ to $\sim10^{-4}$ and 10^{-5} at $F = 5\times10^{-3}$, respectively.

with the perturbation theory results from Eq. (33) denoted by PT and the weak-field asymptotic results from Eq. (41) denoted by WFAT. Equation (33) works well in the whole interval of F considered. The two regimes separated by the field (42) and described by Eqs. (43a) and (44a) can be clearly seen in the upper panels of the figures. In the middle panels, we show the rates $\Gamma_\pm$ divided by the field factors $W_{00}(F, \varkappa_\pm)$, as in the lower panel of Fig. 1. Within the WFAT, the ratio is given by $g_\pm^2$, see Eq. (41). The asymptotic coefficients for the perturbed states (39) vary between the two limits (43b) and (44b) as F passes through F_d, and the dashed lines in the middle panels reproduce this variation. In the present model, g_{2s} and g_{2p} coincide for $\varepsilon = 0$ and remain rather close to each other for small values of ε considered in the figures. Hence g_- and g_+ are close at $F \ll F_d$, but become quite different at $F \gg F_d$, because g_+ is very small there; see Eq. (44b). This results in the characteristic shape of the dashed lines in the middle panels of Figs. 3 and 4. The exact results are seen to demonstrate a similar behavior. However, it is difficult to compare the exact and WFAT results for the + state, because of the small values of g_+ at $F \gg F_d$. To eliminate this drawback of the presentation, in the bottom panels of the figures we plot the rates $\Gamma_\pm$ divided by the WFAT rates $\Gamma_\pm^{(as)}$ defined in Eq. (41). Within the WFAT, the ratio for

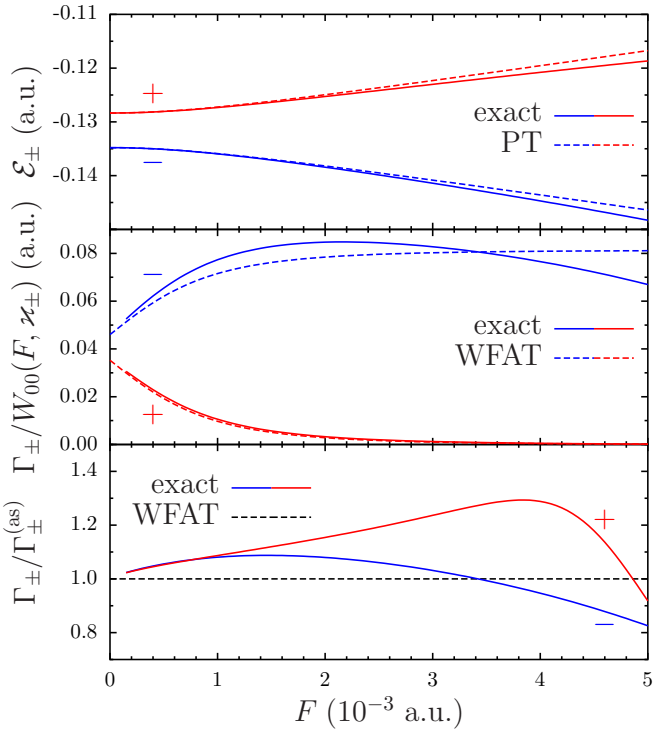

FIG. 4. Same as in Fig. 3, but for the potential (45) with $\varepsilon = 0.2$. In this case $E_{2s} = -0.134\,795$, $E_{2p} = -0.128\,352$, $g_{2s} = 0.2145$, $g_{2p} = 0.1878$, and $d = 2.895$, so $F_d = 1.1\times10^{-3}$. Γ_- and Γ_+ vary from $\sim10^{-261}$ and 10^{-242} at $F = 1.5\times10^{-4}$ to $\sim10^{-5}$ and 10^{-4} at $F = 5\times10^{-3}$, respectively.

both states $\pm$ is equal to 1. Now it is clearly seen that the results from Eq. (41) converge to the exact results at $F \to 0$, and the difference grows approximately linearly with F. This behavior is consistent with the leading-order approximation; a similar behavior is seen from the comparison of the WFAT(0) and exact results in the lower panel in Fig. 1. Importantly, the solid lines in the bottom panels of Figs. 3 and 4 do not exhibit any change in their behavior around the field F_d, as is the case in the top and middle panels, which reflects the fact that the asymptotics (41) is uniform in ΔE.

To close this section, we point out that the present theory holds also in the degenerate case, when $\Delta E = 0$ and $F_d = 0$. Consider, e.g., the hydrogen atom described by the potential (45) with $\varepsilon = 0$. In this case $E_{2s} = E_{2p} = -1/8$, $g_{2s} = g_{2p} = 2^{-5/2}$, and $d = 3$. The correct zeroth-order eigenstates $\psi_-(\mathbf{r})$ and $\psi_+(\mathbf{r})$ of the unperturbed atom are the parabolic states with quantum numbers $(n_\xi, n_\eta, m) = (0, 1, 0)$ and (1,0,0), respectively [1]. From Eq. (44b) we obtain $g_- = 1/4$ and $g_+ = 0$. The value of g_- coincides with the asymptotic coefficient in Eq. (22) for the state (0,1,0), see Ref. [7]; substituting it into Eq. (41), one obtains the correct leading-order WFAT ionization rate of the state [3,4,7]. The zero value of g_+ reflects the fact that the state (1,0,0) ionizes only in channel $\nu = (1, 0)$ which has a higher power of F in the field factor (26), therefore within the leading-order approximation considered here its ionization rate (41) turns to zero. We also mention that the present theory provides the foundation for the treatment of tunneling ionization from the two degenerate orbitals in molecules CH_3F and CH_3Br within the analysis of experimental high-harmonic spectra reported in Ref. [22].

IV. ISOLATED STATE IN DISSOCIATING MOLECULES

We next discuss tunneling ionization of molecules in the process of dissociation, when molecular fragments are already separated by large distances. In this section we consider tunneling ionization from a state which remains isolated as the fragments move away from each other. The solution to this auxiliary problem paves the way for the discussion of tunneling ionization from states which become nearly degenerate at large distances between the fragments presented in the next section.

Before we turn to the derivation, it is worthwhile to explain qualitatively why dissociating molecules require a special consideration. At large distances between the fragments, the state from which tunneling occurs is localized at one of them; let us call it the parent fragment; the other fragments are termed spectators. As an electron is released from the parent fragment by the field and starts moving away, at the initial stage of its motion, when it is still closer to the parent fragment ion than to spectators, it feels the charge of the parent fragment ion. However, as the electron moves farther away, it eventually feels the total charge of the parent molecular ion. The two charges are generally different, because spectators may be charged, as is typically the case, e.g., in Coulomb explosion. The field factor (26), and hence the ionization rate (27), depend on the charge of the parent ion felt by the outgoing electron. The variation of this charge during the release of an electron from a dissociating molecule affects the ionization rate, which is not accounted for by the theory summarized in Sec. II. In this section we show how to incorporate this effect into the WFAT.

To be specific, we consider a heteronuclear diatomic molecule aligned along the field and modeled by the potential

$$V(\mathbf{r}) = Z_p U_a(r) + Z_s U_a(|\mathbf{r} - R\mathbf{e}_z|), \tag{46}$$

where Z_p and Z_s are the nuclear charges, R is the internuclear distance, and

$$U_a(r) = -\frac{1}{\sqrt{r^2 + a^2}} \tag{47}$$

is a soft-core Coulomb potential. We consider tunneling ionization from the ground $1s\sigma$ state in this potential. We use the same notation for the energy $E_0 = -\varkappa^2/2$, wave function $\psi_0(\mathbf{r})$, and dipole moment μ_z of the unperturbed state as in Sec. II. It is assumed that $Z_p > Z_s$, so for large R this state is localized in the potential well created by the nucleus with charge Z_p. This explains the subscripts of Z_p and Z_s which refer to the parent and spectator nuclei, respectively. Taking into account that a shift of the molecule with respect to the coordinate frame does not alter the ionization rate, for convenience we have placed the parent nucleus at the origin. The potential (46) satisfies Eq. (2) with $Z = Z_p + Z_s$. Thus, the charge felt by the electron during its release from the system varies from Z_p to Z. We wish to investigate the effect of this variation on the ionization rate. The effect appears only for sufficiently large R, so a new small parameter $1/R$ emerges in the problem. Our goal is to obtain the weak-field asymptotics of the ionization rate which is uniform in R. Of main interest is the case $R \sim \eta_t = O(F^{-1})$, when the variation of the charge occurs within the interval of η

considered in the derivation of Eq. (27). We therefore consider the asymptotics

$$F \to 0, \quad R = O(F^{-1}). \tag{48}$$

The second relation specifies the term "dissociating molecule" in the present context.

The illustrative calculations in this section are performed with

$$Z_p = 1, \quad Z_s = 0.5, \quad R = 8. \tag{49}$$

The analytical treatment below applies to any values of the softening parameter a in Eq. (47), including the pure Coulomb case $a = 0$. The unperturbed state also can be calculated for any a. In the case $a = 0$ we obtain $E_0 = -0.562\,651$ and $\mu_z = -0.036\,402$. The need of softening is dictated by limitations of a program [27] used to calculate the ionization rate. The present accurate results for the rate are calculated with $a = 0.3$. In this case we obtain $E_0 = -0.471\,019$ and $\mu_z = -0.073\,374$.

In the rest of this section, we first formulate equations which should be considered instead of Eq. (18) for treating tunneling ionization in the present model (Sec. IV A). Then we obtain the large R asymptotics of the asymptotic coefficient in the dominant ionization channel $\nu = (0, 0)$ for the state $\psi_0(\mathbf{r})$ (Sec. IV B) and the weak-field asymptotics of the ionization rate (Sec. IV C).

A. Decoupled equations

In Sec. II, we assumed that in the interval of η where Eq. (15) are to be considered the potential can be substituted by its asymptotic form (2), and hence the matrix (16) vanishes, which has led us to the decoupled equations (18). This is true for compact systems, but may be not the case for systems of large spatial extent. The present potential (46) satisfies Eq. (2) at $r \gg R$, so for sufficiently large R the above assumption ceases to hold. Let us show that in this case one can still neglect the off-diagonal elements of the matrix (16), but must take into account its diagonal elements, which modifies the decoupled equations.

For deriving the ionization rate, we need to consider Eq. (1) in the region $\xi = O(F^0)$, $\eta = O(F^{-1})$. Due to the second of Eqs. (48), this corresponds to the region

$$\xi = O(R^0), \quad \eta = O(R^1). \tag{50}$$

The effective charge (17) for the potential (46) in this region is given by

$$Z(\mathbf{r}) = Z_p + \frac{Z_s\eta}{\eta + 2R} + \frac{Z_s\xi}{\eta + 2R}\left[1 - \frac{\eta(\eta - 2R)}{(\eta + 2R)^2}\right] + O(R^{-2}). \tag{51}$$

The first and second terms here are $O(R^0)$. Their sum varies from Z_p at $\eta \ll 2R$ to Z at $\eta \gg 2R$, and this describes the variation of the charge of the parent ion felt by the outgoing electron. These terms do not depend on ξ or φ and contribute only to the diagonal elements of the matrix (16). The third term in Eq. (51) is $O(R^{-1})$. It contains ξ and hence couples the different parabolic channels. The order of this term upon substituting into Eq. (15) is $O(\eta^{-2})$. We have neglected such terms in Eq. (18) for deriving the leading-order WFAT rate (27) and will do so again in Sec. IV C. However, for the derivation in Sec. IV B, we need to take this term into account. It is sufficient to treat it within the first order of perturbation theory, which amounts to retaining its contribution only to the diagonal elements of the matrix (16). We thus arrive at the decoupled equations

$$\left[\frac{d^2}{d\eta^2} + \frac{F\eta}{4} + \frac{E}{2} + \frac{\beta_\nu(\eta)}{\eta} + \frac{1 - m^2}{4\eta^2}\right] f_\nu(\eta) = 0, \tag{52}$$

where

$$\beta_\nu(\eta) = \beta_\nu - \frac{2Z_sR}{\eta + 2R} + \frac{Z_s\xi_\nu}{\eta + 2R}\left[1 - \frac{\eta(\eta - 2R)}{(\eta + 2R)^2}\right] \tag{53}$$

and

$$\xi_\nu = \langle\Phi_\nu|\xi|\Phi_\nu\rangle. \tag{54}$$

These equations should be solved subject to the same asymptotic boundary conditions (22), for $F = 0$, and (19), for $F > 0$. They should be considered instead of Eq. (18) in the present model. The main difference between the equations stems from the dependence of the separation constants (53) on η. This dependence is caused by the spectator; in the absence of the spectator, $Z_s = 0$, Eq. (52) reduce to Eq. (18).

B. Asymptotic coefficient

Let us begin with the field-free case. The unperturbed state $\psi_0(\mathbf{r})$ is given by Eq. (21), where the coefficient functions satisfy Eq. (52) with $F = 0$ and Eq. (22). We consider only the dominant ionization channel $\nu = (0, 0)$. In this section we derive the asymptotics of the asymptotic coefficient g_{00} for

$$R \to \infty. \tag{55}$$

The derivation reveals the effect of the spectator on the value of g_{00} and yields the function $g_{00}(\eta)$ needed for the next section. We follow a scheme used in Sec. II, namely, we construct inner and outer solutions and match them in an intermediate region, where both solutions apply. The main difference is that the small parameter in the present case is $1/R$ instead of F.

We first construct the inner solution. Consider Eq. (1) in the region $1 \ll r \ll R$. Here, the spectator term in the potential (46) can be treated as a perturbation. We thus obtain

$$E_0 = E_{1s} - \frac{Z_s}{R} - \frac{\alpha Z_s^2}{2R^4} + O(R^{-6}), \tag{56a}$$

$$\mu_z = \frac{\alpha Z_s}{R^2} + O(R^{-4}), \tag{56b}$$

$$\psi_0(\mathbf{r}) = \psi_{1s}(r) + O(R^{-2}), \tag{56c}$$

where E_{1s} and $\psi_{1s}(r)$ are the energy and wave function of the $1s$ state of the parent fragment defined by

$$\left[-\tfrac{1}{2}\Delta + Z_pU_a(r) - E_{1s}\right]\psi_{1s}(r) = 0 \tag{57}$$

and α is its static dipole polarizability. This state satisfies

$$\psi_{1s}(r)|_{r\to\infty} = g_{1s}\sqrt{\frac{\varkappa_{1s}}{2\pi}}(2r)^{Z_p/\varkappa_{1s}-1}e^{-\varkappa_{1s}r}, \tag{58}$$

where $\varkappa_{1s} = \sqrt{-2E_{1s}}$ and g_{1s} is the corresponding asymptotic coefficient. Using Eq. (56c) and the notation (36), we can

present $\psi_0(\mathbf{r})$ in the inner region in the form

$$\psi_0(\mathbf{r})|_{1\ll\eta\ll 2R} = \eta^{-1/2} g_{00}(\eta)\Phi(\xi;\varkappa), \tag{59}$$

where

$$g_{00}(\eta) = g_{1s}\eta^{Z_p/\varkappa-1/2}e^{-\varkappa\eta/2}. \tag{60}$$

We have neglected here the difference between $\varkappa_{1s}$ and $\varkappa = \varkappa_{1s} + Z_s/\varkappa_{1s}R + O(R^{-2})$, which is justified in the region considered. Equation (59) complies with Eq. (21) where only one channel $\nu = (0,0)$ is left. For the potential defined by Eqs. (46) and (49), in the pure Coulomb case $a = 0$ we have $E_{1s} = -0.5, \alpha = 4.5$, and $g_{1s} = \sqrt{2}$. From Eqs. (56) we obtain $E_0 \approx -0.562\,637$ and $\mu_z \approx 0.0352$, which closely agree with the values given below Eq. (49). In the soft-core case $a = 0.3$ we have $E_{1s} = -0.408\,257$, $\alpha = 8.807\,614$, and $g_{1s} = 1.184$. From Eqs. (56) we obtain $E_0 \approx -0.471\,026$ and $\mu_z \approx 0.0688$. The agreement for the dipole moment in this case is worse, which is explained by a more diffuse function $\psi_{1s}(r)$.

We now construct the outer solution in the region (50). It has the same form (59), where the function $g_{00}(\eta)$ is to be found by solving Eq. (52). For $F = 0$, we find from Eq. (54) $\xi_{00} = \varkappa^{-1}$, so the separation constant is given by

$$\beta_{00}(\eta) = Z_p + \frac{Z_s\eta}{\eta+2R} - \frac{\varkappa}{2} + \frac{Z_s}{\varkappa(\eta+2R)}\left[1 - \frac{\eta(\eta-2R)}{(\eta+2R)^2}\right]. \tag{61}$$

To find the asymptotics of $g_{00}(\eta)$ in the limit (55), we employ techniques from asymptotic analysis [31,32]. Introducing a new variable $x = \eta/R$, the equation for $g_{00}(\eta)$ can be written as

$$\left[\frac{d^2}{dx^2} - R^2\rho(x)\right]g_{00}(\eta) = 0, \tag{62}$$

where

$$\rho(x) = \rho_0(x) + R^{-1}\rho_1(x) + R^{-2}\rho_2(x), \tag{63}$$

and

$$\rho_0(x) = \frac{\varkappa^2}{4}, \tag{64a}$$

$$\rho_1(x) = -\frac{Z_p}{x} - \frac{Z_s}{x+2} + \frac{\varkappa}{2x}, \tag{64b}$$

$$\rho_2(x) = -\frac{Z_s}{\varkappa x(x+2)} + \frac{Z_s(x-2)}{\varkappa(x+2)^3} - \frac{1}{4x^2}. \tag{64c}$$

We wish to find the solution to Eq. (62) satisfying the asymptotic boundary condition (22). The solution is sought in the form

$$g_{00}(\eta) = g_{00}R^{Z/\varkappa-1/2}\exp[R\sigma_0(x) + \sigma_1(x) + R^{-1}\sigma_2(x) + O(R^{-2})]. \tag{65}$$

Substituting this ansatz into Eq. (62), we obtain

$$\sigma_0'^2(x) = \rho_0(x), \tag{66a}$$

$$2\sigma_0'(x)\sigma_1'(x) + \sigma_0''(x) = \rho_1(x), \tag{66b}$$

$$2\sigma_0'(x)\sigma_2'(x) + \sigma_1''(x) + \sigma_1'^2(x) = \rho_2(x). \tag{66c}$$

These equations can be easily solved,

$$\sigma_0(x) = -\frac{\varkappa x}{2}, \tag{67a}$$

$$\sigma_1(x) = \left(\frac{Z_p}{\varkappa} - \frac{1}{2}\right)\ln x + \frac{Z_s}{\varkappa}\ln(x+2), \tag{67b}$$

$$\sigma_2(x) = -\frac{Z_pZ_s}{\varkappa^3}\ln\left(\frac{x+2}{x}\right) - \frac{(Z_p-\varkappa)^2}{\varkappa^3 x} - \frac{Z_s(Z_s-2\varkappa)}{\varkappa^3(x+2)} - \frac{2Z_s}{\varkappa^2(x+2)^2}. \tag{67c}$$

Substituting this into Eq. (65) gives

$$g_{00}(\eta) = g_{00}\eta^{Z/\varkappa-1/2}\left(\frac{\eta+2R}{\eta}\right)^{Z_s/\varkappa-Z_pZ_s/\varkappa^3R} e^{-\varkappa\eta/2} \times \exp\left[-\frac{(Z_p-\varkappa)^2}{\varkappa^3\eta} - \frac{Z_s(Z_s-2\varkappa)}{\varkappa^3(\eta+2R)} - \frac{2Z_sR}{\varkappa^2(\eta+2R)^2}\right]. \tag{68}$$

At $\eta \gg 2R$, this function converges to the asymptotic form (22). On the other hand, in the interval $1 \ll \eta \ll 2R$ it takes the form

$$g_{00}(\eta) = g_{00}(2R)^{Z_s/\varkappa-Z_pZ_s/\varkappa^3R}\eta^{Z_p/\varkappa-1/2}e^{-\varkappa\eta/2}, \tag{69}$$

where we have retained only the leading-order terms in $1/\eta$ and η/R. The dependence of this function on η coincides with that of the inner solution (60).

The inner and outer solutions are matched in the region $1 \ll \eta \ll 2R$. By equating the constant factors in Eqs. (60) and (69) we find

$$g_{00} = g_{1s}(2R)^{-Z_s/\varkappa+Z_pZ_s/\varkappa^3R}. \tag{70}$$

This formula gives the asymptotics of g_{00} in the limit (55). The two terms in the power of $2R$ are the leading-order and the first-order terms of the expansion in $1/R$. To derive only the leading-order term it would suffice to neglect in Eq. (52) terms $O(\eta^{-2})$; we retained these terms for obtaining the first-order correction, which considerably improves the accuracy of Eq. (70). A rigorist may notice a seeming inconsistency: $\varkappa$ depends on R and should be also expanded in $1/R$. However, the expansion does not account for exchange terms in the dependence of $\varkappa$ on R for homonuclear molecules, e.g., H_2^+ considered in Sec. V, which decay exponentially in R. As a consequence, it does not distinguish gerade and ungerade states, which reduces the accuracy of Eq. (70).

For the potential defined by Eqs. (46) and (49), in the pure Coulomb $a = 0$ and soft-core $a = 0.3$ cases we obtain from accurate calculations $g = 0.439$ and 0.340, while Eq. (70) predicts the values $g = 0.443$ and 0.343, respectively. In both cases Eq. (70) works pretty well even for the present not very large R.

Equation (70) reveals a strong dependence of g_{00} on R caused by the spectator. Since the ionization rate is proportional to g_{00}^2, this dependence represents one of the effects of the spectator on the rate. The other effect accumulated during tunneling is discussed next.

C. Ionization rate

Here we construct the weak-field asymptotics of the solution to Eq. (52) satisfying the outgoing-wave boundary condition (19) for the dominant ionization channel $\nu = (0, 0)$ and by matching it with the inner solution obtained in the previous subsection find the ionization amplitude f_{00}. Equation (52) is to be considered in the interval $\eta = O(F^{-1})$. We restrict our treatment to the leading-order approximation in F. In this case, it is sufficient to retain only two terms in the expansion for the energy (5a) and neglect the last term in the separation constant (61) and the $O(\eta^{-2})$ term in Eq. (52). The technique of solving Eq. (52) is similar to that used in Refs. [7,8]. Introducing a new variable $y = F\eta/\varkappa^2$, the equation for $f_{00}(\eta)$ can be written as

$$\left[\frac{d^2}{dy^2} + F^{-2}q(y)\right] f_{00}(\eta) = 0, \tag{71}$$

where

$$q(y) = q_0(y) + Fq_1(y) + O(F^2), \tag{72}$$

and

$$q_0(y) = \frac{\varkappa^6}{4}(y-1), \tag{73a}$$

$$q_1(y) = \frac{\varkappa^2}{y}\left[Z - \frac{\varkappa}{2} - \frac{2Z_sRF}{\varkappa^2 y + 2RF}\right] - \frac{\mu_z\varkappa^4}{2}. \tag{73b}$$

The solution is sought in the form

$$f_{00}(\eta) = f_{00}\left(\frac{2}{\varkappa}\right)^{1/2} \exp[iF^{-1}s_0(y) + is_1(y) + O(F^1)]. \tag{74}$$

Substituting this ansatz into Eq. (71), we obtain

$$s_0'^2(y) = q_0(y), \tag{75a}$$

$$2s_0'(y)s_1'(y) - is_0''(y) = q_1(y). \tag{75b}$$

By solving these equations we find

$$s_0(y) = \frac{\varkappa^3}{3}(y-1)^{3/2}, \tag{76a}$$

$$\begin{aligned} s_1(y) = {} & \frac{i}{4}\ln(y-1) - \mu_z\varkappa(y-1)^{1/2} \\ & + \frac{2Z_p - \varkappa}{\varkappa}\arctan(y-1)^{1/2} \\ & + \frac{2\zeta Z_s}{\varkappa}\arctan\zeta(y-1)^{1/2} \\ & - \frac{\pi(2Z_p - \varkappa + 2\zeta Z_s)}{2\varkappa}, \end{aligned} \tag{76b}$$

where

$$\zeta = \frac{\varkappa}{(\varkappa^2 + 2RF)^{1/2}}. \tag{77}$$

Substituting Eqs. (76) into Eq. (74) and setting $y \gg 1$, it can be seen that the solution obtained satisfies Eq. (19). We analytically continue this solution through the upper half of the complex y plane to the region $y < 1$ by substituting $y - 1 = e^{i\pi}(1 - y)$. Setting $y \ll 1$ and returning to the original variable η, we obtain

$$\begin{aligned} f_{00}(\eta) = {} & f_{00}\left(\frac{2}{\varkappa}\right)^{1/2}\left(\frac{F\eta}{4\varkappa^2}\right)^{Z_p/\varkappa - 1/2}\left(\frac{1-\zeta}{1+\zeta}\right)^{\zeta Z_s/\varkappa} e^{-\varkappa\eta/2} \\ & \times \exp\left[\frac{\varkappa^3}{3F} + \mu_z\varkappa + \frac{i\pi}{4} - \frac{i\pi(Z_p + \zeta Z_s)}{\varkappa}\right]. \end{aligned} \tag{78}$$

This form of $f_{00}(\eta)$ holds in the matching region $\eta = O(F^{-1/2})$, where it is seen to coincide with the inner solution (69). Note that Eq. (78) is derived in the leading-order approximation in F, which due to the second of Eqs. (48) corresponds to the leading-order approximation in $1/R$. In this approximation, one should omit the second term in the power of $2R$ in Eq. (69). By matching the inner and outer solutions, we obtain the ionization amplitude

$$\begin{aligned} f_{00} = {} & \frac{g_{00}\varkappa^{1/2}}{2^{1/2}}\left(\frac{4\varkappa^2}{F}\right)^{Z_p/\varkappa - 1/2}(2R)^{Z_s/\varkappa}\left(\frac{1+\zeta}{1-\zeta}\right)^{\zeta Z_s/\varkappa} \\ & \times \exp\left[\frac{i\pi(Z_p + \zeta Z_s)}{\varkappa} - \frac{i\pi}{4} - \varkappa\mu_z - \frac{\varkappa^3}{3F}\right]. \end{aligned} \tag{79}$$

This result should be compared with Eq. (23) for the same channel. First of all, one can see that the amplitudes coincide in the absence of the spectator, $Z_s = 0$, and hence the difference between them is caused by the spectator. An important parameter in the present theory is the product RF. Due to the second of Eqs. (48), this product is treated as a constant. Let us consider the limits of its small and large values. For $RF \ll 1$ we have $\zeta \approx 1 - RF/\varkappa^2$, and it can be seen that Eq. (79) reduces to Eq. (23). This means that as R decreases for a fixed F, the present theory reduces to the theory summarized in Sec. II, which is what one would expect. On the other hand, for $RF \gg 1$ we have $\zeta \ll 1$. In this limit, Eq. (79) again reduces to Eq. (23), but with Z and g_{00} substituted by Z_p and $g_{00}(2R)^{Z_s/\varkappa} \approx g_{1s}$, respectively; see Eq. (70). This means that as R grows for a fixed F, the present theory reduces to that of Sec. II applied to the parent fragment, as if there is no the spectator, which is also expectable. Summarizing, Eq. (79) gives the weak-field asymptotics of f_{00} which is uniform in R.

Using Eq. (79), we obtain the ionization rate

$$\Gamma \approx \left(\frac{RF}{2\varkappa^2}\right)^{2Z_s/\varkappa}\left(\frac{1+\zeta}{1-\zeta}\right)^{2\zeta Z_s/\varkappa} G_{00}^2 W_{00}(F, \varkappa). \tag{80}$$

This formula generalizes Eq. (27) for the present model. The difference between the two formulas is represented by the first two factors in Eq. (80). As explained above, these factors turn to unity as $F \to 0$ for a fixed R. We illustrate the performance of Eq. (80) for the model defined by Eqs. (46) and (49) in the soft-core case $a = 0.3$. We consider only the ionization rate. The results for the rate divided by the field factor $W_{00}(F, \varkappa)$ are plotted in Fig. 5. The exact rate is compared with the asymptotic results from Eqs. (27) and (80) denoted by WFAT and WFAT-R, respectively. The former formula gives for the ratio shown in the figure a constant value $G_{00}^2 \approx 0.133$. The latter formula converges to this limiting value at $F \to 0$.

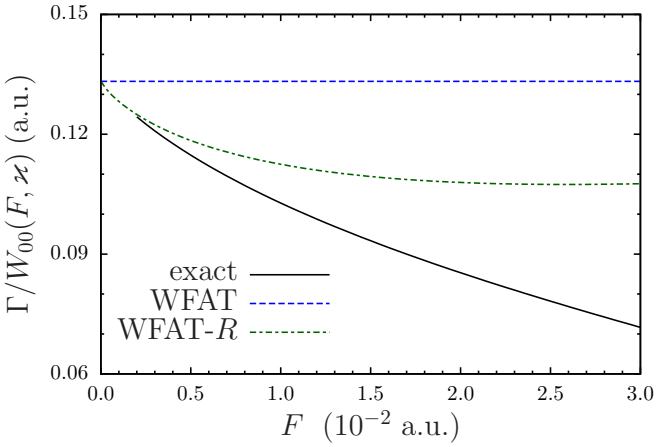

FIG. 5. Ionization rate of the $1s\sigma$ state in the potential (46) with the parameters (49) in the soft-core case $a = 0.3$ divided by the field factor $W_{00}(F,\varkappa)$. The solid (black) line shows results of accurate calculations. The dashed (blue) and dash-dotted (green) lines show the WFAT results from Eqs. (27) and (80), respectively. The rate Γ varies from $\sim 10^{-127}$ at $F = 2\times10^{-3}$ to $\sim 10^{-6}$ at $F = 3\times10^{-2}$.

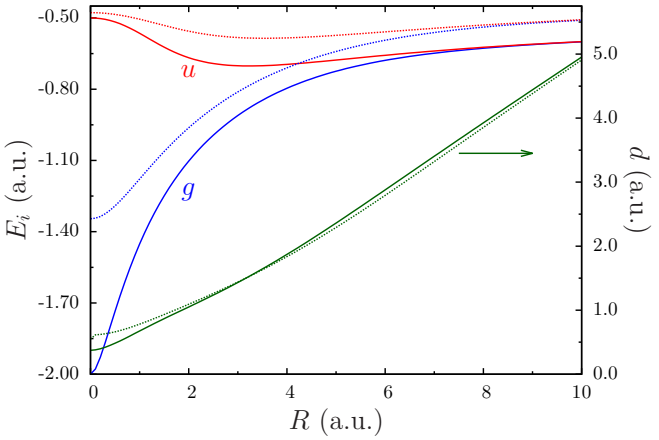

FIG. 6. Energies of the $1s\sigma_g$ and $2p\sigma_u$ bound states in the potential (81) (left axis) denoted by g and u and associated with states 1 and 2 from Sec. III, respectively, and the dipole matrix element (32) between the states (right axis) as functions of the internuclear distance. Solid and dotted lines show results for the pure Coulomb ($a = 0$) and soft-core ($a = 0.3$) potentials, respectively.

The exact results also approach this limiting value, but in a way different from that seen in Fig. 1, not linearly. Equation (80) reproduces the characteristic behavior of the exact results and at all fields works better than Eq. (27). For the present value of $R = 8$, the product RF is less than 0.24 in the interval of fields considered, so we are in the regime where Eq. (80) is still rather close to Eq. (27). To test Eq. (80) in the opposite regime $RF \gg 1$ we would have to drastically increase R, since F should satisfy the condition (28). Unfortunately, we cannot do this because of limitations of the program [27] used for calculating the exact rate. The task of validation of Eq. (80) in the case $RF \gg 1$ remains for future studies.

The following comment is in order here. In the model considered in this section, tunneling occurs from a state localized at the lower nucleus. In this case, the electron does not meet the spectator during or after tunneling. For the opposite orientation of the same molecule with respect to the field, the electron would have to pass through the spectator. In this case, the ionization rate may be affected by the mechanism of resonant tunneling ionization [34] proceeding via static-field-induced states [35] of the spectator. The present treatment does not account for this mechanism.

V. NEARLY DEGENERATE STATES IN DISSOCIATING MOLECULES

In this section, we combine the theories developed in Secs. III and IV and apply them to the analysis of tunneling ionization from a pair of gerade and ungerade states of a dissociating homonuclear diatomic molecule which are nearly degenerate at large internuclear distances. The molecule is modeled by the potential

$$V(\mathbf{r}) = U_a(r) + U_a(|\mathbf{r} - R\mathbf{e}_z|), \tag{81}$$

which corresponds to Eq. (46) with $Z_p = Z_s = 1$. In the pure Coulomb case $a = 0$ this potential describes the hydrogen molecular ion H_2^+. To comply with the formulation of Sec. IV in order to be able to use the results obtained therein, we have placed the lower nucleus at the origin. We consider tunneling ionization from the $1s\sigma_g$ and $2p\sigma_u$ states in this potential. For brevity, these states will be denoted by g and u. We associate them with states 1 and 2 from Sec. III, respectively, and use the notation introduced therein. Let us emphasize that the notation is defined in the coordinate frame of Eq. (81). The unperturbed energies $E_1 = E_g$ and $E_2 = E_u$ of the states and the dipole matrix element d between them as functions of the internuclear distance R calculated for two values of the softening parameter a are shown in Fig. 6. Their numerical values for the pure Coulomb case $a = 0$ are given in Table I. The dipole moments (31) are $\mu_g = \mu_u = -R/2$. The signs of the unperturbed wave functions $\psi_i(\mathbf{r})$ are fixed by the condition $\psi_i(\mathbf{0}) > 0$; then the asymptotic coefficients $g_1 = g_g$ and $g_2 = g_u$ and the dipole matrix element d are positive. For the present system $Z = 2$. The states under consideration become degenerate at $R \to \infty$; the difference between their energies $\Delta E = E_u - E_g$ decays exponentially in R. Our goal is to describe tunneling ionization in the case of small ΔE and simultaneously large R.

It is more conventional to consider homonuclear diatomics in the geometrical center frame. Some of the quantities involved in the analysis, e.g., the unperturbed energies E_i, the dipole matrix element d, and the ionization rate Γ, do not depend on the frame, but some others do. The real part of the SS energy (3) and the asymptotic coefficients in Eq. (22) do depend on the frame. In the illustrative calculations below, for convenience of the reader, we present the results for the asymptotic coefficients in the dominant ionization channel $\nu = (0,0)$ of the unperturbed states $\psi_i(\mathbf{r})$ and the energies of the perturbed states $\pm$ in the geometrical center frame, denoting them by $g_i^{(c)}$ and $\mathcal{E}_\pm^{(c)}$, respectively. They are related to the corresponding quantities g_i and $\mathcal{E}_\pm$ in the frame used in Eq. (81) by the transformations

$$g_i^{(c)} = g_i e^{\varkappa_i R/2}, \tag{82a}$$

$$\mathcal{E}_\pm^{(c)} = \mathcal{E}_\pm - RF/2. \tag{82b}$$

TABLE I. Characteristics (in atomic units) of the unperturbed $1s\sigma_g$ and $2p\sigma_u$ states of H_2^+ [pure Coulomb potential (81) with $a = 0$] denoted by g and u, respectively, needed for calculating the ionization rates (85). E_g and E_u are the energies of the states, $g_g^{(c)}$ and $g_u^{(c)}$ are their asymptotic coefficients in the dominant ionization channel $\nu = (0, 0)$ in the geometrical center frame, and d is the dipole matrix element, Eq. (32).

R	E_g	E_u	$g_g^{(c)}$	$g_u^{(c)}$	d
0	−2.0	−0.5	2.8284	0.70711	0.37247
1	−1.451 786	−0.564 814	2.6455	0.88625	0.67490
2	−1.102 634	−0.667 534	2.6155	1.3436	1.0499
3	−0.910 896	−0.701 418	2.7946	1.9171	1.4327
4	−0.796 085	−0.695 551	3.2180	2.6267	1.8709
5	−0.724 421	−0.677 292	3.9613	3.5713	2.3607
6	−0.678 636	−0.657 311	5.1455	4.8926	2.8791
7	−0.648 451	−0.639 129	6.9563	6.7942	3.4043
8	−0.627 570	−0.623 606	9.6816	9.5787	3.9259
9	−0.612 307	−0.610 655	13.767	13.702	4.4420
10	−0.600 579	−0.599 901	19.901	19.861	4.9535
11	−0.591 208	−0.590 934	29.131	29.106	5.4619
12	−0.583 502	−0.583 391	43.117	43.102	5.9682
13	−0.577 027	−0.576 983	64.389	64.380	6.4730
14	−0.571 498	−0.571 480	96.891	96.885	6.9768
15	−0.566 716	−0.566 709	146.76	146.75	7.4798
16	−0.562 536	−0.562 534	223.57	223.56	7.9823
17	−0.558 851	−0.558 850	342.30	342.29	8.4843
18	−0.555 578	−0.555 577	526.43	526.42	8.9860
19	−0.552 649	−0.552 649	812.84	812.84	9.4875
20	−0.550 014	−0.550 014	1259.6	1259.6	9.9887

The numerical values of $g_i^{(c)}$ for the pure Coulomb case are given in Table I. The error of these results is ∼1%. However, this error is partially canceled in the difference $g_g^{(c)} - g_u^{(c)}$ defining g_+ at large F, see Eq. (44b), so we give the values of $g_i^{(c)}$ with five significant digits.

We begin with the asymptotic coefficients. Formula (70) was obtained for an isolated state localized at the lower nucleus. In the present homonuclear case, the unperturbed state densities $\psi_i^2(\mathbf{r})$ at large R are equally distributed between the nuclei, so the coefficient g_{1s} in Eq. (70) defined by Eq. (58) should be substituted by $g_{1s}/\sqrt{2}$. We thus obtain

$$g_i = \frac{g_{1s}}{\sqrt{2}}(2R)^{-1/\varkappa_i + 1/\varkappa_i^3 R}. \tag{83}$$

In Fig. 7, we compare the exact results for $g_i^{(c)}$ (coinciding with the results given in Table I) with the asymptotic results obtained from Eqs. (82a) and (83) for the pure Coulomb case. The asymptotic results are seen to quickly converge to the exact ones as R grows. Note that it becomes prohibitively difficult to accurately calculate the asymptotic coefficients for large R. Figure 7 shows that in this case one can use Eq. (83).

The amplitudes of ionization $f_\pm$ in the dominant ionization channel $\nu = (0, 0)$ for the states $\pm$ in the present model can be obtained by combining the derivations presented in Secs. III and IV. The inner solutions given by Eq. (38) should be matched in the region $\eta = O(F^{-1/2})$ with the outer solutions given by Eq. (78), where $\varkappa$ should be substituted by $\varkappa_\pm$.

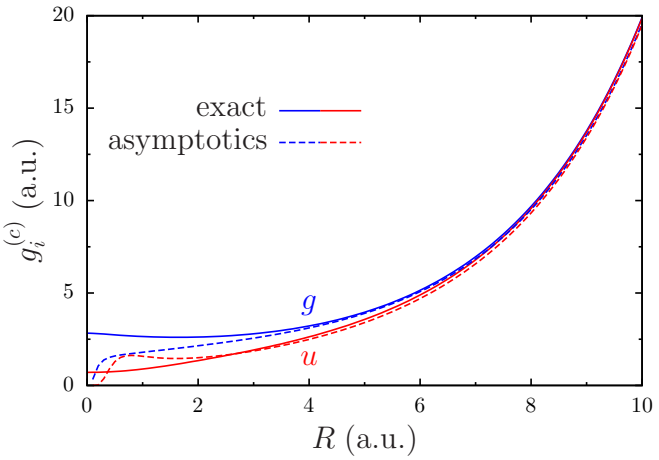

FIG. 7. Asymptotic coefficients $g_g^{(c)}$ and $g_u^{(c)}$ [in the geometrical center frame, see Eq. (82a)] in the dominant ionization channel $\nu = (0, 0)$ for the $1s\sigma_g$ and $2p\sigma_u$ states of H_2^+ denoted by g and u, respectively, as functions of the internuclear distance. Solid lines show results of accurate calculations. Dashed lines show the large R asymptotic results obtained from Eqs. (82a) and (83).

Omitting further details, the result is

$$f_\pm = \frac{g_\pm \varkappa_\pm^{1/2}}{2^{1/2}} \left(\frac{4\varkappa_\pm^2}{F}\right)^{1/\varkappa_\pm - 1/2} (2R)^{1/\varkappa_\pm} \left(\frac{1+\zeta_\pm}{1-\zeta_\pm}\right)^{\zeta_\pm/\varkappa_\pm} \times \exp\left[\frac{i\pi(1+\zeta_\pm)}{\varkappa_\pm} - \frac{i\pi}{4} - \frac{\varkappa_\pm^3}{3F}\right]. \tag{84}$$

Here $\zeta_\pm$ is defined by Eq. (77) with $\varkappa$ substituted by $\varkappa_\pm$. The corresponding rates are

$$\Gamma_\pm \approx \left(\frac{RF}{2\varkappa_\pm^2}\right)^{2/\varkappa_\pm} \left(\frac{1+\zeta_\pm}{1-\zeta_\pm}\right)^{2\zeta_\pm/\varkappa_\pm} \Gamma_\pm^{(\mathrm{as})}, \tag{85}$$

where $\Gamma_\pm^{(\mathrm{as})}$ is defined by Eq. (41). This formula combines the generalizations of Eq. (27) represented by Eqs. (41) and (80).

We have calculated the energies and ionization rates of the states $\pm$ in a soft-core potential (81) with $a = 0.3$. The results as functions of F for two representative internuclear distances $R = 4$ and 8 are shown in Figs. 8 and 9. It is instructive to compare the present model with the model discussed in Sec. III. The behavior of the energies is similar to that seen in Figs. 3 and 4. One can clearly distinguish two regimes separated by the field (42) in which the difference between $\mathcal{E}_\pm^{(c)}$ remains almost constant, at $F < F_d$, and begins to grow linearly, at $F > F_d$, in agreement with Eq. (33). The perturbation theory results from Eq. (33) denoted by PT closely reproduce this behavior. The exact rates are compared with the weak-field asymptotic results from Eqs. (41) and (85) denoted by WFAT and WFAT-R, respectively. The behavior of the ratio shown in the middle panels of the figures differs from that shown in the middle panels of Figs. 3 and 4. The difference becomes clear by comparing the − state in Figs. 3 and 9, which correspond to the smaller ΔE in each model. According to Eq. (41), the WFAT result for the ratio is g_-^2, and hence the ratio is expected to become constant at $F > F_d$. This agrees with the behavior of the exact results in Fig. 3, but the exact results in Fig. 9 behave differently and are more closely reproduced by the WFAT-R results from

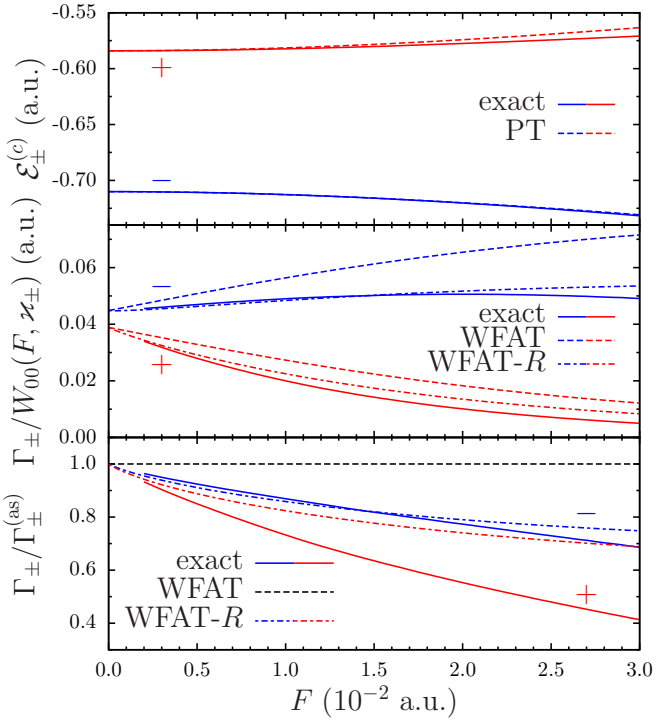

FIG. 8. Energies $\mathcal{E}_\pm^{(c)}$ [in the geometrical center frame, see Eq. (82b)] and ionization rates $\Gamma_\pm$ divided by the field factors $W_{00}(F,\varkappa_\pm)$, in the middle panel, and the WFAT rates $\Gamma_\pm^{(as)}$ defined in Eq. (41), in the bottom panel, as functions of field for the $\pm$ states in a soft-core potential (81) with $a = 0.3$ at the internuclear distance $R = 4$. Solid lines show results of accurate calculations. Dashed lines in the upper panel show the perturbation theory results from Eq. (33). Dashed and dash-dotted lines in the middle and bottom panels show the WFAT results from Eqs. (41) and (85), respectively. Γ_- and Γ_+ vary from $\sim 10^{-237}$ and 10^{-174} at $F = 2\times10^{-3}$ to $\sim 10^{-11}$ and 10^{-6} at $F = 3\times10^{-2}$, respectively.

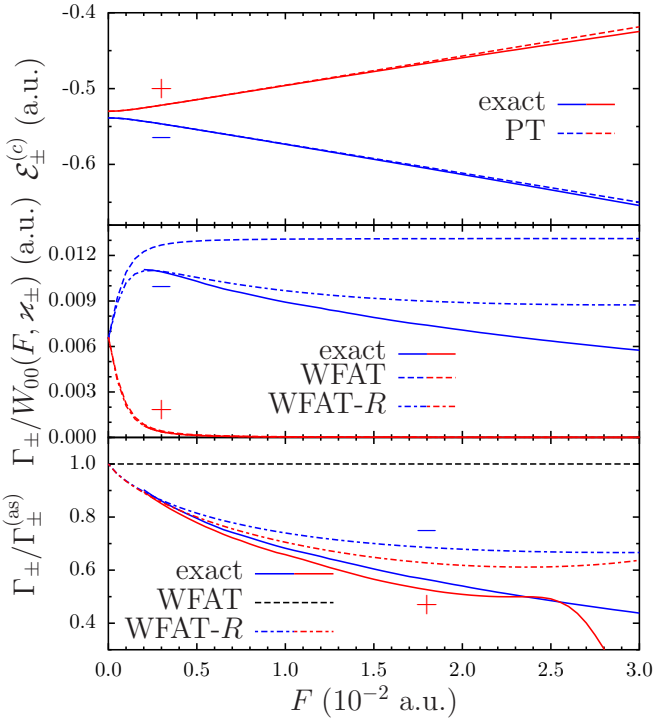

FIG. 9. Same as in Fig. 8, but for $R = 8$. Γ_- and Γ_+ vary from $\sim 10^{-153}$ and 10^{-146} at $F = 2\times10^{-3}$ to $\sim 10^{-7}$ and 10^{-3} at $F = 3\times10^{-2}$, respectively.

Eq. (85). The difference between the two models with nearly degenerate states becomes especially clear, now for both states $\pm$, by comparing the bottom panels in Figs. 3 and 9. While the exact results in Fig. 3 linearly approach unity at $F \to 0$, and this behavior is similar to that seen in the bottom panel of Fig. 1, the exact results in Fig. 9 demonstrate a characteristic behavior similar to that seen in Fig. 5. This difference is caused by the large spatial extent of the present system. Equation (85), which accounts for this difference, works better for both states than Eq. (41), which does not.

Let us return to the comment made in the end of Sec. IV. At large R and simultaneously sufficiently large F, as is the case for $R = 8$ at $F > 5\times10^{-3}$, see Fig. 9, the $-$ and $+$ states in the present system are localized near the bottom and top nuclei, respectively. Figure 9 shows that the present theory correctly describes tunneling ionization from both these states. However, while for the $-$ state the ratio shown in the bottom panel of Fig. 9 (solid blue line) behaves smoothly, for the $+$ state this ratio (solid red line) begins to rapidly vary at $F > 2.5\times10^{-2}$. This variation is caused by an avoided crossing of the $1s$ state at the upper nucleus, whose energy goes up as F grows, with the $2s$ and $2p$ states at the bottom nucleus, whose energies go down. For the present soft-code model $E_{1s} \approx -0.408$, $E_{2s} \approx -0.113$, and $E_{2p} \approx -0.123$, so the location of the avoided crossing can be estimated as $F \approx (E_{2p} - E_{1s})/R \approx 3.6\times10^{-2}$. A similar avoided crossing in the $2p\sigma$ state of HeH^{2+} was discussed in Ref. [33]. As has been pointed out above, tunneling ionization from the $+$ (upper) state near the avoided crossing is affected by the mechanism of resonant tunneling [34], which is not accounted for by the present theory.

In Fig. 10 we show the dependence of the energies and rates of the same states in the same model on the internuclear distance R at a fixed field $F = 0.01$. The exact results are compared with the different approximations in the same way as in Figs. 8 and 9. As can be seen from Fig. 6 and Table I, the dipole matrix element d grows linearly in R at large internuclear distances. Taking this into account, Eq. (33) predicts that the difference between the perturbed energies $\mathcal{E}_\pm^{(c)}$ approximately coincides with the unperturbed energy distance $\Delta E = E_u - E_g$ at sufficiently small R, where $\Delta E > 2dF$, and begins to grow linearly at larger R, where $\Delta E < 2dF$. This is confirmed by the exact results shown in the top panel of the figure. In the middle and bottom panels the exact rates are compared with the weak-field asymptotic results from Eqs. (41) and (85). For both states $\pm$ in the whole interval of R considered, the asymptotics (85) which accounts for the large extent of the system works better than the one (41) which does not, and this is the main feature to be observed from the figure. The agreement of Eq. (85) with the exact results should improve at larger R, however, to check this is beyond our current computational resources.

The results shown in Figs. 8–10 validate Eq. (85) for a soft-core potential (81) with $a = 0.3$. However, this formula

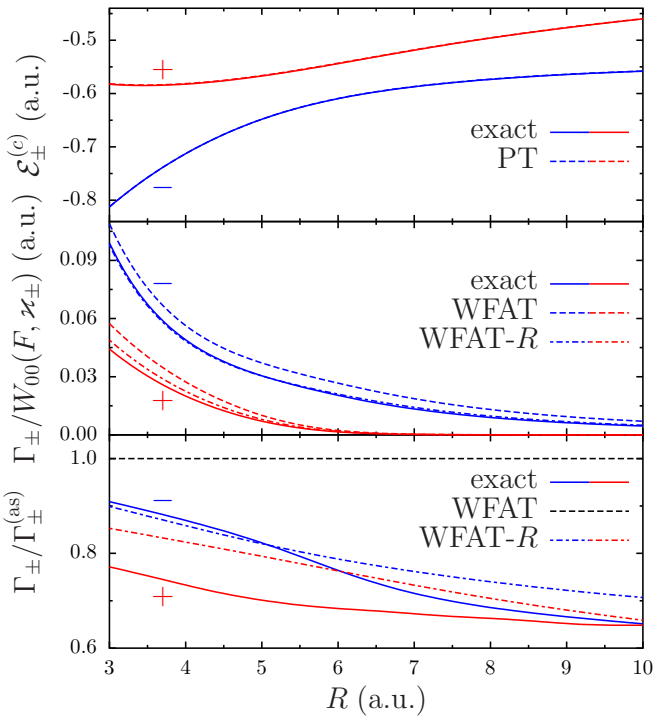

FIG. 10. Similar to Figs. 8 and 9, but the results are shown as functions of the internuclear distance R at a fixed field $F = 0.01$. Γ_- and Γ_+ vary from $\sim 10^{-54}$ and 10^{-29} at $R = 3$ to $\sim 10^{-25}$ and 10^{-20} at $R = 10$, respectively.

holds for any a, including the pure Coulomb case $a = 0$, which corresponds to $H_2{}^+$. Since this molecular ion is often considered as a prototypical molecular system in strong-field physics, we give in Table I numerical values of its characteristics needed to implement Eq. (85). The interval of R where the data are presented is limited by difficulties in calculating the asymptotic coefficients $g_i^{(c)}$.

Let us close this discussion by a comment regarding the phase of the ionization amplitudes (84). In contrast to Eq. (23), where the phase is constant, the first term in the exponent in Eq. (84) depends on both F and R. It is known that the phase must be included in modeling high-order harmonic spectroscopy [22,23], and hence can be extracted from experimental data. Its variation with F and R may thus result in observable effects.

VI. CONCLUSION

The main results of this paper are presented by Eqs. (41), (80), and (85) generalizing the previously known WFAT rate formula (27) to situations characterized by the appearance of an additional small parameter in the tunneling problem. Equation (41) gives the weak-field asymptotics of the ionization rates from states separated by a small energy distance ΔE in a compact system. The asymptotics is uniform in ΔE and converges to Eq. (27) for sufficiently large ΔE, when the states can be treated as isolated. The physical effect accounted for by Eq. (41) is the mixing of nearly degenerate states by the ionizing field. Equation (80) gives the weak-field asymptotics of the ionization rate from an isolated state in a heteronuclear diatomic molecule at large internuclear distances R. The asymptotics is uniform in R and converges to Eq. (27) for sufficiently small R, when the system becomes compact. The physical effect accounted for by Eq. (80) is the variation of an effective parent ion charge felt by the electron as it tunnels and moves away from the molecule. Equation (85) describes tunneling ionization from the nearly degenerate $1s\sigma_g$ and $2p\sigma_u$ states of a homonuclear molecular ion $H_2{}^+$ at large internuclear distances. In this system, both effects mentioned above are present. The effects considered essentially modify the dependence of the ionization rate on the field strength comparing to that predicted by Eq. (27). Formulas (41), (80), and (85) correctly describe the modifications, as confirmed by the illustrative calculations presented. We believe that these formulas will find applications in strong-field physics, as Eq. (27) did.

ACKNOWLEDGMENTS

This work was supported by the Ministry of Education and Science of Russia (State Assignment No. 3.873.2017/4.6) and the Russian Foundation for Basic Research (Grant No. 17-02-00198). T.M. acknowledges support from Japan Society for the Promotion of Science KAKENHI Grants No. 16H04029, No. 16H04103, and No. 17K05597. T.M. also thanks L. Yue for useful discussion.

[1] L. D. Landau and E. M. Lifshitz, *Quantum Mechanics (Non-relativistic Theory)* (Pergamon Press, Oxford, 1977).

[2] B. M. Smirnov and M. I. Chibisov, The breaking up of atomic particles by an electric field and by electron collisions, Zh. Eksp. Teor. Fiz. **49**, 841 (1965) [Sov. Phys. JETP **22**, 585 (1966)].

[3] S. Yu. Slavyanov, Application of the method of standard comparison problems to perturbations of the Coulomb field. The discrete spectrum, Probl. Mat. Fiz. **4**, 125 (1970) [English translation: *Topics in Mathematical Physics* (Consultants Bureau, New York, 1971), Vol. 4, p. 113].

[4] T. Yamabe, A. Tachibana, and H. J. Silverstone, Theory of the ionization of the hydrogen atom by an external electrostatic field, Phys. Rev. A **16**, 877 (1977).

[5] R. J. Damburg and V. V. Kolosov, An asymptotic approach to the Stark effect for the hydrogen atom, J. Phys. B **11**, 1921 (1978).

[6] H. J. Silverstone, E. Harrell, and C. Grot, High-order perturbation theory of the imaginary part of the resonance eigenvalues of the Stark effect in hydrogen and of the anharmonic oscillator with negative anharmonicity, Phys. Rev. A **24**, 1925 (1981).

[7] O. I. Tolstikhin, T. Morishita, and L. B. Madsen, Theory of tunneling ionization of molecules: Weak-field asymptotics including dipole effects, Phys. Rev. A **84**, 053423 (2011).

[8] V. H. Trinh, O. I. Tolstikhin, L. B. Madsen, and T. Morishita, First-order correction terms in the weak-field asymptotic theory of tunneling ionization, Phys. Rev. A **87**, 043426 (2013).

[9] O. I. Tolstikhin, L. B. Madsen, and T. Morishita, Weak-field asymptotic theory of tunneling ionization in many-electron atomic and molecular systems, Phys. Rev. A **89**, 013421 (2014).

[10] V. H. Trinh, O. I. Tolstikhin, and T. Morishita, Weak-field asymptotic theory of tunneling ionization: benchmark analytical results for two-electron atoms, J. Phys. B **48**, 061003 (2015).

[11] V. H. Trinh, O. I. Tolstikhin, and T. Morishita, First-order correction terms in the weak-field asymptotic theory of tunneling ionization in many-electron systems, J. Phys. B **49**, 195603 (2016).

[12] I. I. Fabrikant and G. A. Gallup, Semiclassical propagation method for tunneling ionization, Phys. Rev. A **79**, 013406 (2009).

[13] G. A. Gallup and I. I. Fabrikant, Semiclassical complex-time method for tunneling ionization: Molecular suppression and orientational dependence, Phys. Rev. A **81**, 033417 (2010).

[14] V. I. Osherov and V. G. Ushakov, Stark problem in terms of the Stokes multipliers for the triconfluent Heun equation, Phys. Rev. A **88**, 053414 (2013).

[15] H. Mera, T. G. Pedersen, and B. K. Nikolić, Nonperturbative Quantum Physics from Low-Order Perturbation Theory, Phys. Rev. Lett. **115**, 143001 (2015).

[16] F. Krausz and M. Ivanov, Attosecond physics, Rev. Mod. Phys. **81**, 163 (2009).

[17] O. I. Tolstikhin and T. Morishita, Adiabatic theory of ionization by intense laser pulses: Finite-range potentials, Phys. Rev. A **86**, 043417 (2012).

[18] D. Dimitrovski, T. P. Grozdanov, E. A. Solov'ev, and J. S. Briggs, Ionization and excitation of the hydrogen atom by an electric pulse, J. Phys. B **36**, 1351 (2003).

[19] B. Piraux, F. Mota-Furtado, P. F. O'Mahony, A. Galstyan, and Yu. V. Popov, Excitation of Rydberg wave packets in the tunneling regime, Phys. Rev. A **96**, 043403 (2017).

[20] M. Ohmi, O. I. Tolstikhin, and T. Morishita, Analysis of a shift of the maximum of photoelectron momentum distributions generated by intense circularly polarized pulses, Phys. Rev. A **92**, 043402 (2015).

[21] T. Morishita and O. I. Tolstikhin, Adiabatic theory of strong-field photoelectron momentum distributions near a backward rescattering caustic, Phys. Rev. A **96**, 053416 (2017).

[22] P. M. Kraus, O. I. Tolstikhin, D. Baykusheva, A. Rupenyan, J. Schneider, C. Z. Bisgaard, T. Morishita, F. Jensen, L. B. Madsen, and H. J. Wörner, Nat. Commun. **6**, 7039 (2015).

[23] P. M. Kraus, B. Mignolet, D. Baykusheva, A. Rupenyan, L. Horný, E. F. Penka, G. Grassi, O. I. Tolstikhin, J. Schneider, F. Jensen, L. B. Madsen, A. D. Bandrauk, F. Remacle, and H. J. Wörner, Measurement and laser control of attosecond charge migration in ionized iodoacetylene, Science **350**, 790 (2015).

[24] T. Endo, A. Matsuda, M. Fushitani, T. Yasuike, O. I. Tolstikhin, T. Morishita, and A. Hishikawa, Imaging Electronic Excitation of NO by Ultrafast Laser Tunneling Ionization, Phys. Rev. Lett. **116**, 163002 (2016).

[25] Y. Ito, M. Okunishi, T. Morishita, O. I. Tolstikhin, and K. Ueda, Rescattering photoelectron spectroscopy of heterodiatomic molecules with an analytical returning photoelectron wave packet, Phys. Rev. A **97**, 053411 (2018).

[26] B. Wolter, M. G. Pullen, M. Baudisch, M. Sclafani, M. Hemmer, A. Senftleben, C. D. Schröter, J. Ullrich, R. Moshammer, and J. Biegert, Strong-Field Physics with Mid-IR Fields, Phys. Rev. X **5**, 021034 (2015).

[27] P. A. Batishchev, O. I. Tolstikhin, and T. Morishita, Atomic Siegert states in an electric field: Transverse momentum distribution of the ionized electrons, Phys. Rev. A **82**, 023416 (2010).

[28] L. Hamonou, T. Morishita, and O. I. Tolstikhin, Molecular Siegert states in an electric field, Phys. Rev. A **86**, 013412 (2012).

[29] V. N. T. Pham, O. I. Tolstikhin, and T. Morishita, Molecular Siegert states in an electric field. II. Transverse momentum distribution of the ionized electrons, Phys. Rev. A **89**, 033426 (2014).

[30] *Handbook of Mathematical Functions*, edited by M. Abramowitz and I. A. Stegun (Dover, New York, 1972).

[31] F. W. J. Olver, *Asymptotics and Special Functions* (Academic Press, New York, 1974).

[32] M. V. Fedoryuk, *Asymptotic Analysis: Linear Ordinary Differential Equations* (Springer, Berlin, 1993).

[33] V. H. Trinh, V. N. T. Pham, O. I. Tolstikhin, and T. Morishita, Weak-field asymptotic theory of tunneling ionization including the first-order correction terms: Application to molecules, Phys. Rev. A **91**, 063410 (2015).

[34] W.-C. Jiang, O. I. Tolstikhin, L.-Y. Peng, and Q. Gong, Static-field-induced states and their manifestation in tunneling ionization dynamics of molecules, Phys. Rev. A **85**, 023404 (2012).

[35] A. V. Gets and O. I. Tolstikhin, Static-field-induced states, Phys. Rev. A **87**, 013419 (2013).